

## MODE-I DELAMINATION CHARACTERISATION OF CROSS-PLY FIBER-METAL LAMINATES

J. Laliberté<sup>1</sup>, P. V. Straznicky<sup>1</sup>, and C. Poon<sup>2</sup>

<sup>1</sup>Department of Mechanical and Aerospace Engineering, Carleton University,  
1125 Colonel By Drive, Ottawa, ON, K1S 5B6 CAN

<sup>2</sup>Institute for Aerospace Research, National Research Council of Canada, 1500  
Montreal Road, BLDG M-14, Ottawa, ON, K1A 0R6 CAN

### ABSTRACT

A series of delamination characterisation tests have been carried out on cross-ply fiber-metal laminates (FMLs). These tests were carried out to improve the accuracy of low-velocity impact finite element simulations with a potential new aircraft material. Three variants of the commercially available material known as GLARE (GLASS REinforced) aluminum laminates were employed. These tests were conducted using a modified double-cantilever beam (DCB) test specimen. The results showed that the Mode-I energy release rate ( $G_{IC}$ ) has limited dependence on the lay-up of the FML. A modified data reduction scheme was developed to reduce the static load data to  $G_{IC}$  values. This scheme gave lower values than several other data-reduction methods because it accounted for the deformation of the adherends in the DCB specimens. Fiber-bridging was observed during the DCB tests, however, since the same phenomenon is observed in the impact simulations the  $G_{IC}$  data could still be applied to the simulations.

### KEYWORDS

Fiber-metal laminate, delamination, finite element modelling, fiber-bridging, GLARE, energy release rate

### INTRODUCTION

Fiber-metal laminates (FMLs) are a relatively new class of aerospace materials that consist of metal layers and fiber-reinforced polymer layers bonded together [1, 2 and 3]. Structures manufactured from these materials can benefit greatly from the laminates' increased strength, reduced density and increased resistance to different forms of damage compared to monolithic aluminum. Carleton University, in partnership with the National Research Council of Canada's (NRCC) Institute for Aerospace Research (IAR) and Bombardier Aerospace has been investigating the impact damage resistance of traditional composites and these new hybrid materials [4, 5 and 6]. Currently a finite element (FE) model of low-velocity impact damage in FMLs is being developed. Figure 1 shows the behaviour of the LS-DYNA explicit FE simulation without accounting for the effect of fiber bridging. As can be seen, there is exaggerated deformation and delamination damage. Although there is some data available in literature on the Mode I delamination behaviour of unidirectional FMLs [7] there is none on the behaviour of cross-ply FMLs. Finite element simulations have shown that Mode I behaviour dominates the propagation of the delamination damage in low velocity impact of GLARE. The subsequent sections of this paper will describe the characterisation of the Mode I (opening) delamination behaviour of cross-ply GLARE variants.

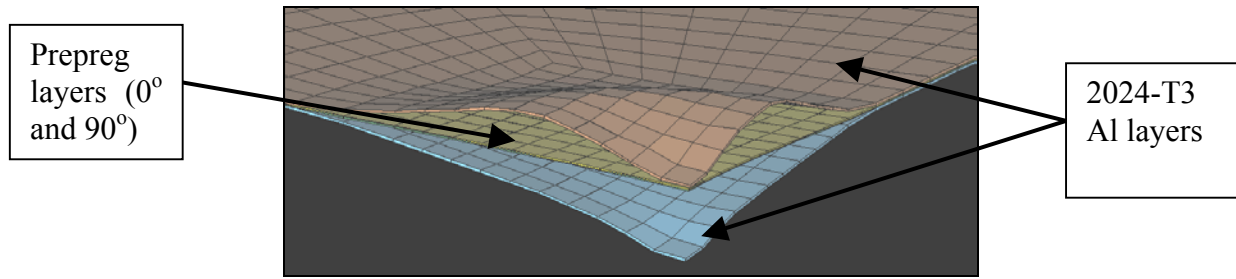


**Figure 1:** Low velocity impact simulation of GLARE without fiber-bridging correction.

## DELAMINATION TESTING OF FIBER-METAL LAMINATES

Interlaminar cracking or delamination is a significant failure mode in fiber-metal laminates. The presence of delamination has been shown to influence the initiation and propagation of fatigue damage [8 and 9]. Delamination propagation in FMLs can be influenced by geometry, material discontinuities and typically consists of coupled Mode I, II and III fracture behaviours defined as opening, in-plane shear and transverse in-plane shear. Finite element modelling of the full structural situation can then provide estimates of the relative contributions of each damage mode. For instance, in FML impact simulations Mode II dominates at the outset of impact and Mode I dominates during the impactor rebound phase. Thus Mode II properties are important for initiation and Mode I behaviour influences the ensuing delamination propagation. It is therefore important to study each mode separately before attempting to combine them in an FE model.

While delamination testing has been carried out on traditional composite materials by numerous other researchers comparatively little work has been conducted with FMLs. This research has mainly centred on delamination in adhesively bonded FML splice joints as well as delamination resulting from crack propagation [7, 10, 11, 12, 13 and 14]. A modified double cantilever beam (DCB) test specimen (Figure 2) was employed by Vlot and van Ingen [7] to determine the Mode I  $G_{IC}$  properties of unidirectional variants of GLARE. The data reduction method used by Vlot and van Ingen was based on classical beam bending theory combined with considerations for the rotation of the two arms at the delamination crack tip. Several other schemes for determining the value of  $G_{IC}$  from experiments are summarised in Table 1. The area method and modified area method use the area enclosed by the segments of the load-displacement curve shown in Figure 3. The modified area method contains corrections that are explained below. The displacement method uses the crosshead displacement and the crack opening displacement to find  $G_{IC}$ . Finally the compliance method uses the relationship between the compliance ( $C$ ) of the specimen and the crack tip displacement ( $a$ ). Readers are directed to the references for the full derivation of the formulae.

TABLE 1  
SUMMARY OF DCB DATA REDUCTION METHODS.

Method	$G_{IC}$ Formula	Ref.
<b>Modified Area Method</b>	$G_{IC} = \frac{P^2}{bE_{11}^*I^*} \left[ a^2 + \frac{2a}{\lambda} + \frac{1}{\lambda^2} \right]$ (1)	15
<b>Area method</b>	$G_{IC} = \frac{4P^2 a^2}{bE_x I_x}$ (2)	15
<b>Displacement Method</b>	$G_{IC} = \frac{3P\delta}{2ba}$ (3)	16
<b>Compliance Method</b>	$G_{IC} = \frac{P^2}{2b} \frac{dC}{da}$ (4)	16

In Table 1  $P$  is the applied load,  $a$  is the crack length,  $I_x$  is the moment of inertia in the axial direction of the beam,  $I^*$  is the modified moment of inertia calculated using the constituent properties,  $E$  is the modulus of the material under consideration,  $E_{11}^*$  is the modified modulus calculated from the constituent properties,  $C$  is the compliance of the specimen (also  $\delta/P$ ),  $\delta$  is the crosshead displacement,  $\lambda$  is defined below, and  $b$  is the width of the specimen.

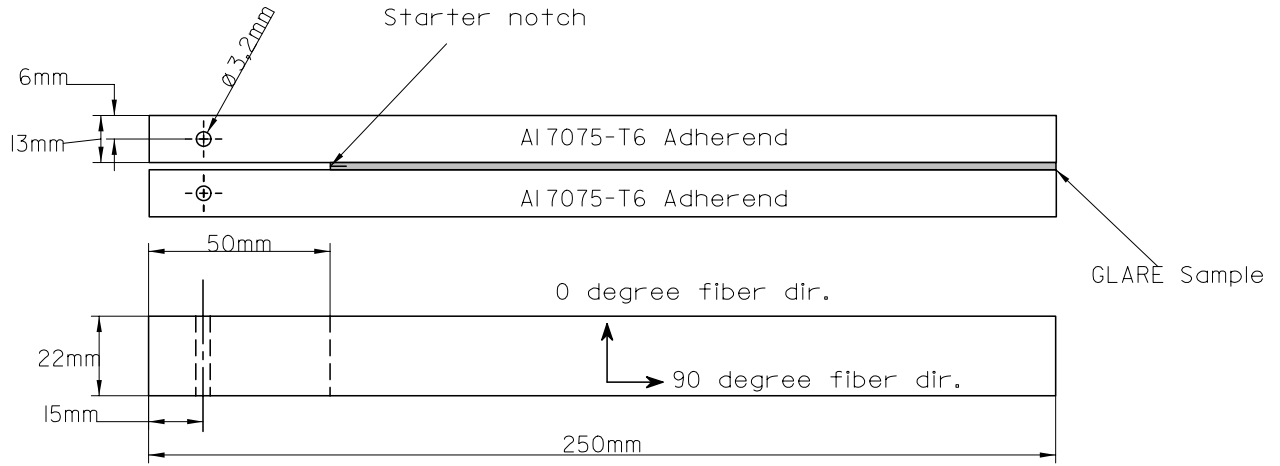


**Figure 2:** DCB specimen configuration.

The modified area method was developed by Kanninen [15] and presented in terms of the stress intensity factor. This relationship can be further modified to yield the Mode I energy release rate,  $G_{IC}$ . Vlot and van Ingen [7] applied this relationship to the results of their experimental testing. The test method employed for the tests described herein employs repeated loading and unloading cycles, which is different than that employed by Vlot and van Ingen. The modified area method is then used to calculate the energy released during the delamination propagation. This method takes into account the curvature of the DCB arms through the application of simple beam theory. The governing differential equation for the deflection,  $w$ , of the beam is:

$$\frac{d^4 w}{dx^4} + 4\lambda^4 H(x)w = 0 \quad (5)$$

where

$$H(x) = \begin{cases} 1, & x > 0 \\ 0, & x < 0 \end{cases}, \quad \lambda = \left[ \frac{k}{4E_{11}^* I^*} \right]^{1/4} \quad \text{and} \quad k = \frac{2bE_{22}}{h}$$

Where  $E_{22}$  is the modulus in the transverse modulus and  $h$  is the height of the specimen. From the solution of this differential Eqn. 5 a relationship for the specimen compliance can be developed that leads to the strain energy for the specimen,  $W$ . The stress intensity factor,  $K$ , can be related to the energy release rate for constant displacement as (Crews and Reeder [17]):

$$K^2 = -\frac{E}{b} \frac{dW}{da} = -2EG_{IC} \quad (6)$$

Substituting in the solution of Eqn. 5 and simplifying yields the relationship shown in Eqn. 1 in Table 1.

## EXPERIMENTAL TESTING

### *Apparatus and DCB Specimen*

Three variants GLARE were employed for these tests. The lay-ups were GLARE-3-2/1 [Al/(0°/90°)/Al], GLARE-4-2/1 [Al/(0°/90°/0°)/Al] and GLARE-5-2/1 [Al/(0°/90°/90°/0°)/Al]. The ply angles are relative to the long axis of the DCB specimen (Figure 2). These particular variants of GLARE were selected in order to study the effect of lay-ups on Mode-I delamination behaviour. Also, there was a lack of published data concerning the Mode-I behaviour of these materials and LS-DYNA impact modelling required this data to accurately simulate the impact events. Earlier durability testing at NRCC made extensive use of these materials [3]. The specimens were prepared as shown in Figure 2. The specimen was loaded in an MTS hydraulic load frame through pins inserted in the holes near the end of the specimen. A 5 mm starter notch was introduced in the FML specimen using a diamond saw. They were then loaded quasi-statically at a rate of 5 mm/min under displacement control until the first evidence of cracking occurred on the load curve. The load was then reduced to zero at the same rate. This procedure was repeated several times for each specimen until complete failure. The amount of crack propagation during each loading step was recorded.

### *Results*

A sample load versus crosshead displacement curve is shown in Figure 3. Each loading repetition is shown on the graph. The initial and final crack tip displacement was recorded for each load step. The final  $G_{IC}$  results are summarised in Table 2 for all of the GLARE variants, averaged for each specimen group (5 specimens per group). The differences in the values calculated using the three different methods will be discussed in the subsequent section.

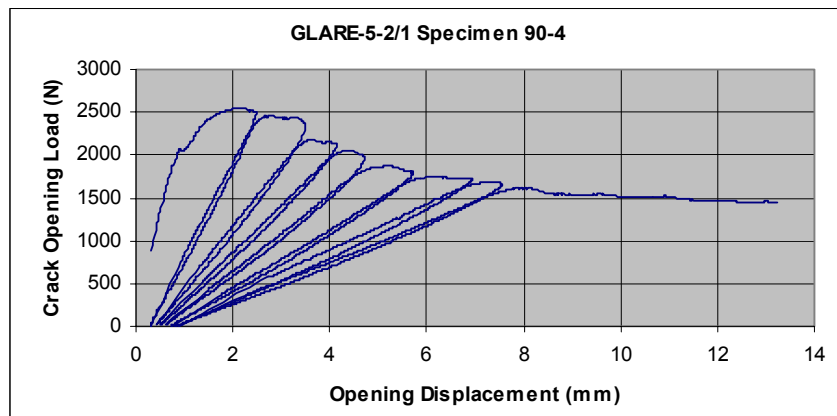


**Figure 3:** Sample load curve from Mode-I delamination characterisation test.

TABLE 2  
MEASURED OF  $G_{IC}$  VALUES

Material	Average Measured $G_{IC}$ Values		
	Modified Area [17]	Area [16]	Displacement [16]
	N/mm	N/mm	N/mm
GLARE-3	1.71	2.50	2.55
GLARE-4	2.24	3.13	2.46
GLARE-5	2.34	3.48	3.54

Extensive fiber bridging was also noted following examinations of the fracture surface of the specimens (Figure 4 and Figure 5a). The delamination cracks propagated in prepreg layers with the fiber oriented parallel to the delamination direction. Each of the three types of GLARE exhibited the same behaviour. This indicates that the “path of least resistance” through the prepreg layer is parallel to the fibers rather than perpendicular. The fibers pull away from the matrix and produce the fracture surface shown in Figure 4.

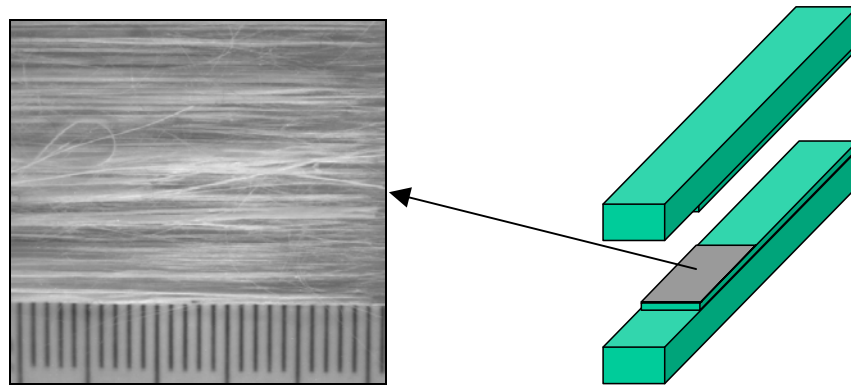


**Figure 4:** Optical micrograph of the “hairy” failure surface in a typical FML DCB specimen.

It is well documented that fiber bridging affects the measured  $G_{IC}$ . Other phenomena, such as crack jumping between layers influence this property as well. However, if the material exhibits the same damage modes in its final application as observed in coupon tests then the results can be applied to the full-scale structure.

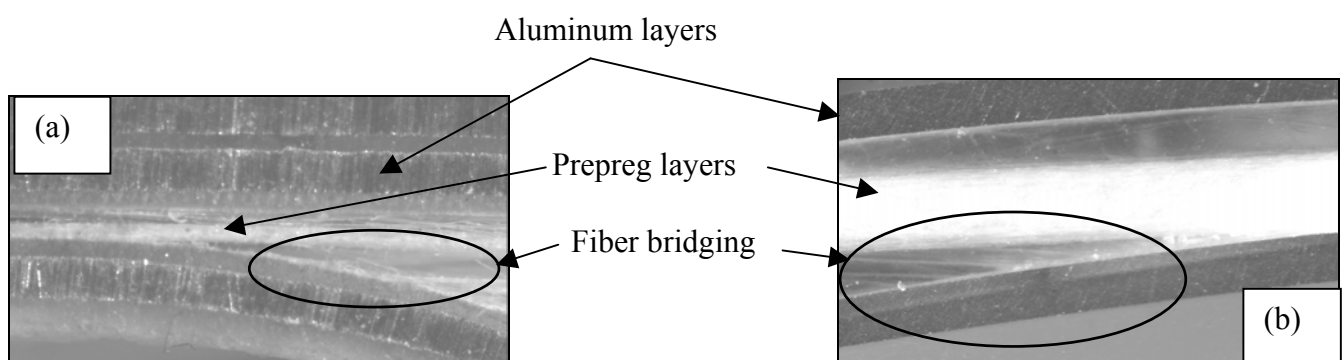


**Figure 5:** (a) Fiber bridging in a typical FML DCB specimen and (b) in an impacted FML specimen.

### ***Discussion of Results***

The differences between the  $G_{IC}$  values calculated by each of the methods in Table 2 can be attributed to the assumptions made in the development of the data reduction methods, specifically:

- The modified area method contains corrections for the bending of the adherends. The flexibility of the adherends affects the measured load-displacement response of the DCB specimen. Also, some of the energy stored in the specimen is stored as elastic strain energy in the aluminum adherends.
- The area method does not take the specimen flexibility into consideration and thus produces a higher calculated value of  $G_{IC}$ .
- The displacement method is based on the measured crack opening displacement of the specimen. There is no direct accounting for the stiffness of the specimen or the adherends. As with the area method this results in a  $G_{IC}$  that includes strain energy effects of the specimen and also the load frame if an extensometer is not used to measure the crack opening displacement.

### **MODELLING OF DELAMINATION DAMAGE IN FMLS**

Following the completion of the DCB testing the results were then employed to generate crack opening load curves that relate the crack opening stress to the displacement. This information was used to improve the LS-DYNA low velocity impact simulations described earlier. The resulting behaviour more closely resembles that observed in the experimental low-velocity impact tests (Figure 6a and Figure 6b). LS-DYNA simulations were generated of the DCB specimens. By applying the load values measured during the DCB experiments to the FE simulations it was possible to develop a preliminary load versus displacement curve incorporating the effects of fiber bridging.

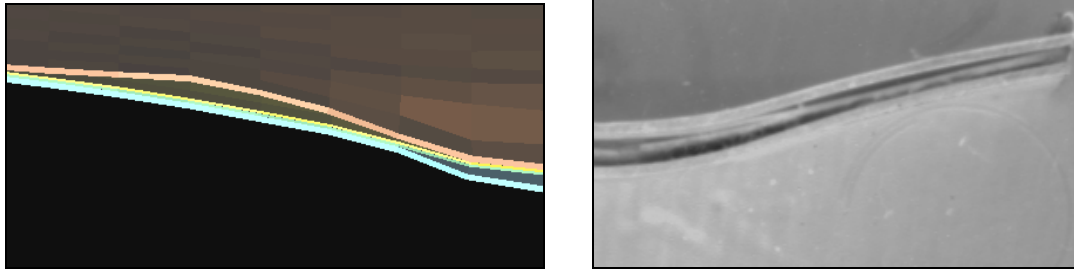


**Figure 6:** (a) Corrected low velocity impact simulation result (b) impacted FML specimen.

## CONCLUSIONS AND FUTURE WORK

The Mode-I delamination behaviour of several GLARE cross-ply laminates has been investigated using double cantilever beam specimens. The data from the tests were reduced to  $G_{IC}$  using three different techniques. Differences between the  $G_{IC}$  results were explained based on the formulation of the data reduction methods. Fiber bridging was noted in the DCB specimens, however the same damage mode was observed in impacted specimens. Therefore, the  $G_{IC}$  data is valid provided the damage modes between the coupon tests and the final structure are the same. Since this is the case with the experimental impact simulations the DCB test results are applicable to the LS-DYNA simulations. The LS-DYNA simulations were successfully improved in accuracy using the DCB test data.

The next phase in this research will involve estimating the energy released during impact by measuring the delaminated area. Knowing the  $G_{IC}$  for the material will allow a comparison between the experimental value of absorbed energy and the FE derived value.

## ACKNOWLEDGEMENTS

The authors would like to thank Tom Benak and Tony Marincak of NRCC for their invaluable and dedicated technical assistance with the experimental test portion of this project. Sincere gratitude is also due Katherine McCuaig, a senior undergraduate student from Carleton University who provided much assistance to the development of the DCB specimens and test methodology. Bombardier Aerospace also provided financial assistance through the NRC-Bombardier Collaborative FML Durability Project (NRC Project number 46-QJO\_18).

## REFERENCES

1. Lawcock, G., Ye, L. and Mai, Y-W. (1995) *SAMPE Journal* 31, 23.
2. Asundi, A. and Choi, Alta Y.N. (1997) *J. Mat. Processing Technology* 63, 386.
3. Laliberté, J., Poon, C. and Straznicky, P.V. (1999) IAR LTR-ST-2231, NRC Canada.
4. Veitinghoff, H. E. (1994) MEng Thesis, Carleton University, Canada.
5. Majeed, R. O. (1995) MEng Thesis, Carleton University, Canada.
6. Fouss, E. O. (1996) MEng Thesis, Carleton University, Canada.
7. Vlot, A. and van Ingen, J. W. (1998) *J. Composite Mat.* 32, 1805.
8. Li, K., Chudnovosky, A., Kin, Y and Macheret, J. (1995) *Poly. Composites* 15, 52.
9. Li, E. and Johnson, W. S. (1998) *J. Composites Tech. and Research* 20, 3.
10. Yeh, J. R. (1988) *Eng. Fract. Mech.* 30, 827.
11. Vries, T.J. de, Vlot, A. and Hashagen, F. (1999) *Composite Struct.* 46, 131.
12. Lin, C.T. and Kao, P.W. (1996) *Acta Materialia* 44, 1181.
13. Hashagen, F., de Borst, R. and de Vries, T. (1999) *Composite Struct.* 46, 147.
14. Guo, Y.J., Wu, X.R. and Zhang, Z.L. (1997) *Fatigue Fract. Eng. Mat. Struct.* 20, 1699.
15. Kanninen, M. F. (1973) *Int. J. Fract.* 9, 83.
16. Hashemi, S., Kinloch, A., Williams, J. (1989) *J. Mat. Sci. Letters* 8, 125.
17. Crews, J.H. and Reeder, J. R., NASA TM 100662, 1988.